Monthly Notices
of the
ROYAL ASTRONOMICAL SOCIETY

MNRAS **482,** 4096–4110 (2019)
Advance Access publication 2018 October 25

doi:10.1093/mnras/sty2704

Orbits of 14 binaries based on 2018 SOAR speckle observations

José A. Docobo,[1,2,3]★ Jorge Gomez,[1,2]★ Pedro P. Campo,[1,2]★ Manuel Andrade,[1,2,4] Elliott P. Horch,[5,6] Edgardo Costa[7] and Rene A. Mendez[7]

[1]*Observatorio Astronómico Ramón María Aller, Universidade de Santiago de Compostela (USC), Avenida das Ciencias s/n, Campus Vida, Santiago de Compostela, E-15782 Galiza, Spain*
[2]*Instituto de Matemáticas and Departamento de Matemática Aplicada, Facultade de Matemáticas, USC, Rúa Lope Gómez de Marzoa, s/n, Campus Vida, Santiago de Compostela, E-15782 Galiza, Spain*
[3]*Real Academia de Ciencias de Zaragoza, Facultad de Ciencias, C/ Pedro Cerbuna 12, E-50009 Zaragoza, Spain*
[4]*Escola Politécnica Superior de Enxe naría, USC, Benigno Ledo s/n, Campus Terra, Lugo, E-27002 Galiza, Spain*
[5]*Department of Physics, Southern Connecticut University, 501 Crescent Street, New Haven, CT 06515, USA*
[6] *Lowell Observatory, 1400 W. Mars Hill Rd., Flagstaff, AZ 86001, USA*
[7]*Universidad de Chile, Casilla 36-D Santiago, Chile*

Accepted 2018 October 2. Received 2018 October 1; in original form 2018 June 16

ABSTRACT

New data obtained during the 2018 March–April speckle run at the 4.1 m Southern Astrophysical Research (SOAR) telescope located at Cerro Pachón (Chile) allowed us to recalculate the orbits of the following visual binaries: WDS 06478+0020 (STT 157), WDS 07003−2207 (FIN 334Aa,Ab), WDS 07013−0906 (A 671), WDS 10174−5354 (CVN 16Aa,Ab), WDS 12155−3106 (RST 1658), WDS 12572+0818 (FIN 380), WDS 13044−1316 (HU 642), WDS 14243−3838 (RST 1785), WDS 16094−3103 (I 557), WDS 17115−1630 (HU 169), WDS 17119−0151 (LPM 629), WDS 17563 + 0259 (A 2189), WDS 18464−2755 (RST 2073), and WDS 19035−6845 (FIN 357). All but three of them are Southern stars. The recently published *Gaia* parallaxes were used to calculate the total mass of each of these systems, despite the fact that, in a few cases, only *Hipparcos* parallaxes were available. For two binaries, A 671 and RST 2073, there are no parallax data. However, in these cases, the masses deduced from the dynamical parallaxes provided relevant information. In addition, we also present the first orbit for each of three systems: HU 642, RST 1785, and RST 2073, using speckle measurements. Finally, using the dynamical parallaxes given by these orbits, we have been able to calculate the luminosity of these systems. Said luminosities allow us to indicate an approximate age for each of the components of the system, situating them within the HR diagram.

Key words: techniques: high angular resolution – astrometry – binaries: visual – stars: fundamental parameters.

1 INTRODUCTION

The recently published *Gaia* (Gaia Collaboration 2016, 2018) high precision parallaxes entail calculating orbital parameters of binary systems with the highest accuracy in order to obtain reliable stellar masses. In this way, dedicated instrumentation designed to implement high resolution techniques such as speckle interferometry (Labeyrie 1970) with large telescopes is the most suitable mode to obtain the best results.

The 4.1 m SOAR telescope located at Cerro Pachón (Chile) has proved to be a very useful instrument to perform high resolution measurements of close binaries. In fact, when equipped with the HRCam (Tokovinin & Cantarutti 2008), it allows for interferometry combined with adaptive optics yielding resolutions in the 0.012–3.37 arcsec range. Regarding rms of the calibration in a typical observing run, 0.°1–0.°2 and 0.002–0.004 are estimated in the orientation and in the scale, respectively. In addition, differential photometry data (Δm) are also obtained during this procedure.

SOAR speckle runs were specifically designed to collect a large quantity of relevant data from both well-known and less-known systems, even from those with undetected subcomponents (Tokovinin 2018a). As a matter of fact, these data were used in orbital calculations (e.g. Mendez et al. 2017; Tokovinin 2017; Mason et al. 2018; Tokovinin 2018b) and, consequently, in the precise determination of stellar masses and dynamical parallaxes.

The HRCam, a fast imager designed to work either as a standalone instrument or with the SOAR Adaptive Module, SAM

★ E-mail: joseangel.docobo@usc.es (JAD); jorge.gomez2@rai.usc.es (JG); pedropablo.campo@usc.es (PPC)

(Tokovinin et al. 2016), was used in all of those observational runs. Improvements in acquisition systems and data processing have yielded a constant increase in the number of results per year (Tokovinin et al. 2015; Tokovinin 2016; Tokovinin et al. 2018) as well as demonstrated the intensive work that is being carried out by the SOAR speckle group with the aim to increase the number of measurements and the quality of the samples of Southern orbits.

On the other hand, the well-known analytic method of Docobo (1985, 2012) was used to calculate the orbits. This versatile method is based on a mapping from the interval $(0, 2\pi)$ into the set of Keplerian orbits whose corresponding apparent orbits pass through three base points $(\theta_i, \rho_i ; t_i)$ $(i = 1, 2, 3)$. In contrast to the Thiele-Innes-van den Bos method, knowledge of the areal constant is not necessary. In a recent paper, Docobo, Tamazian & Campo (2018) explained the different selection criteria for the orbit: the solution with minimal rms of the O–C residuals from all of the weighted observations, matching dynamical and trigonometric (*Gaia* or *Hipparcos*) parallaxes, and/or the agreement between the calculated masses and those that correspond to the spectral types.

This investigation is a collaboration between the research group of the Universidad de Chile and the Ramon Maria Aller Astronomical Observatory, Universidade de Santiago de Compostela, for the investigation of binary and multiple stellar systems in the context of the IAU G1 Commission. The observation time was allocated by the Chilean National Time Allocation Committee (program CN2018A-1). A detailed description of the procedure for processing data is described in Tokovinin et al. (2018).

The astrometric monitoring of the binary systems, especially those with short periods, is essential to achieve definitive orbits as soon as possible. Likewise, those with an evident orbital motion should be systematically observed by means of speckle interferometry. Binary systems measured in this observational run were chosen on the basis of various scientific criteria: systematic deviations of the O–C residuals, binaries with few or any high resolution records, binaries without parallax data, orbits providing unrealistic masses, systems of special astrophysical interest, etc.

We have used measurements of the SOAR 2018 speckle run to calculate the 14 orbits presented in this work. In addition, the whole set of speckle measurements available in the Fourth Catalogue of Interferometric Measurements of Binary Stars (Mason et al. 2001) as well as the historical data base of micrometric measurements Worley (1997) have also been used. The weights assigned to each type of measurement are those shown in Docobo & Ling (2003).

After this introduction, we present the results and discussion with individual comments for each binary in Section 2 (figures showing the recalculated orbits along with the available observations are also included). Following the detailed comments regarding each system, we have included a final section in which we calculate the luminosities and the ages of the systems. Using the luminosities of the system, we are able to plot their location in the HR diagram together with the isochrones calculated using the metallicity data of the system when available or the metallicity of the Sun, otherwise. To create these plots, we used the metallicity data obtained from Gaidos et al. (2014), Ammons et al. (2006), Anderson & Francis (2012), and the effective temperature provided by Gray (2005). We inferred the temperature for the stellar spectra that are not explicitly included there. The data used are presented in Table 7. One diagram per system is provided where different isochrones generated with MESA Isochrones and Stellare Tracks (Paxton et al. 2011, 2013, 2015; Choi et al. 2016; Dotter 2016) are displayed against the position of the system components in the HR diagram (Figs 17–30). Conclusions are discussed in Section 3.

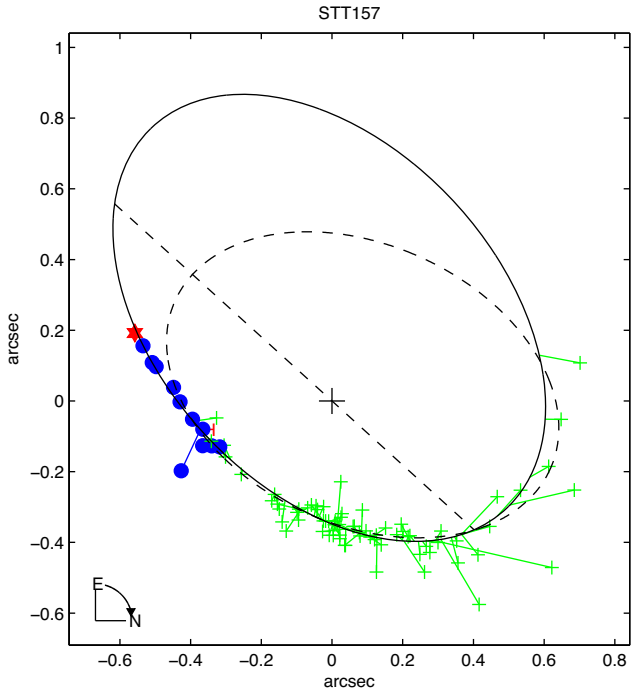

Figure 1. Following ORB6 standards, the micrometric observations are plotted as green crosses, *Hipparcos* as H, the speckle observations are identified by blue circles, and the latest ones obtained by SOAR are designated with the ⋆ symbol. All of these symbols are united by their respective colour line to the new orbit, joining the real observation with its expected position according to the time of observation. The previous apparent orbit is represented by a dashed black line and our new apparent orbit by a solid line. The line of nodes is traced by a straight dashed line upon which the position of the primary star can be seen as a large cross. The left corner arrow is used to indicate the direction of the orbital movement. The new orbit of STT 157 (the longer period orbit) is compared to the previous one.

The new orbits presented in this paper are indicated with a solid line and the immediately previous orbit, with a broken line. All the details related with the plots can be read in the Fig. 1 caption.

2 RESULTS AND DISCUSSION

In Tables 1 and 2, each system is identified by a WDS number (Mason et al. 2001) and by the discoverer code (name of the binary) in the first column. For each binary displayed within Table 1, we list the corresponding orbital elements with their standard errors (columns 2–8): period (in years), epoch of the periastron passage (in Besselian and Julian years), eccentricity, semimajor axis (in arcseconds), inclination (in degrees), angle of the node (in degrees), and argument of the periastron (in degrees). We also include the correction for precession used to refer the angles of position to the standard equinox of J2000.0 (column 9). In addition, the epoch of the last observation that was used for orbit calculation appears in the same column. Table 2 provides the ephemerides for the next 5 yr with the θ values in degrees and those of ρ in arcseconds.

Table 3 shows the magnitudes, spectral types, parallaxes, and the calculated masses in the following format. In column 1, the WDS number and the *Hipparcos* identifier (ESA 1997) appear. The name of the binary is listed in column 2. The apparent magnitudes for each component are found in columns 3 and 4. These values are preferably taken from the WDS Catalogue (Mason et al. 2001). In the case that they do not exist in said Catalogue, they can also be

Table 1. Orbital elements. When both, short period orbits marked with ∗ and long period with ∗∗.

WDS name	P(yr) σ	T(B1950.0) σ T(J2000.0)	e σ	a(arcsec) σ	i(°) σ	Ω(°) σ	ω(°) σ	Prec. (°) last obs
06478+0020	500.0	1958.3	0.400	0.781	129.4	137.8	238.4	0.0018
STT157	±100.0	±3.5	±0.1	±0.1	±5.0	±5.0	±5.0	2018.2352
		1958.3						
07003−2207	102.87	1980.21	0.859	0.112	124.3	86.1	292.4	0.0054
FIN334Aa,Ab∗	±9.13	±3.24	±0.016	±0.018	±6.7	±6.9	±1.6	2018.2491
		1980.21						
07003−2207	1000.	2012.	0.739	0.444	106.3	153.2	171.2	0.0054
FIN334Aa,Ab∗∗	±200.0	±5.27	±0.039	±0.044	±3.0	±3.0	±3.0	2018.2491
		2012.						
07013−0906	159.49	1965.15	0.741	0.314	132.4	112.3	115.2	0.0063
A671∗	±3.5	±2.85	±0.03	±0.015	±2.6	±4.7	±4.8	2018.2491
		1965.15						
07013−0906	342.00	1889.00	0.081	0.453	115.8	159.6	348.9	0.0063
A671∗∗	±24.0	±21.0	±0.009	±0.01	±2.5	±3.4	±21.1	2018.2491
		1889.00						
10174−5354	5.347	2016.711	0.123	0.096	13.1	134.1	99.4	0.0106
CVN16Aa,Ab	±0.007	±0.015	±0.003	±0.002	±2.5	±15.0	±15.0	2018.2355
		2016.709						
12155−3106	62.00	2047.37	0.226	0.680	51.4	116.9	240.7	− 0.0059
RST1658	±0.2	±0.2	±0.003	±0.004	±0.5	±0.5	±1.0	2018.2356
		2047.37						
12572+0818	55.00	2023.61	0.877	0.235	86.4	164.9	120.8	0.0125
FIN380	±0.38	±0.3	±0.012	±0.09	±0.5	±0.5	±1.5	2018.2357
		2023.61						
13044−1316	660.	1955.	0.408	0.705	106.9	47.5	124.8	0.0016
HU642AB	±80.0	±2.0	±0.057	±0.048	±1.0	±1.0	±2.2	2018.2361
		1955.						
14243−3838	92.34	1987.77	0.220	0.222	45.3	60.7	65.2	0.0005
RST1785	±1.2	±0.22	±0.006	±0.002	±1.0	±1.0	±2.0	2018.2523
		1987.77						
16094−3103	136.20	2034.00	0.726	0.620	85.9	26.3	248.4	0.0061
I557	±10.0	±3.0	±0.080	±0.050	±1.0	±1.0	±4.5	2018.2359
		2034.00						
17115−1630	79.08	1992.00	0.452	0.223	124.4	22.0	61.8	0.0038
HU169	±0.08	±0.2	±0.006	±0.005	±1.0	±1.0	±1.0	2018.2499
		1992.00						
17119−0151	34.64	2023.09	0.160	0.753	14.7	170.8	193.3	− 0.0038
LPM629	±0.200	±1.050	±0.010	±0.008	±2.5	±5.0	±10.0	2018.2363
		2023.09						
17563+0259	171.73	1975.08	0.517	0.235	71.0	150.8	328.3	0.0056
A2189	±6.17	±0.72	±0.02	±0.008	±1.0	±1.0	±2.0	2018.2555
		1975.08						
18464−2755	243.5	1983.0	0.544	0.406	128.0	130.6	214.0	0.0054
RST2073	±13.5	±0.28	±0.03	±0.015	±1.5	±2.5	±3.0	2018.25
		1983.0						
19035−6845	14.050	2018.226	0.385	0.142	163.5	101.9	193.9	− 0.0139
FIN357	±0.06	±0.04	±0.003	±0.001	±0.5	±1.5	±1.5	2018.2554
		2018.224						

deduced using the SIMBAD (Wenger et al. 2000) total magnitude as well as the magnitude difference yielded by SOAR speckle observations. The same thing occurs with the spectral types that appear in columns 5 and 6. Preferably, we use the WDS data. If not, the individual spectral types were obtained from the composite spectrum taking into account the difference of magnitude calculated for the system (more details below). The *Gaia* or *Hipparcos* parallaxes (van Leeuwen 2007) and the total mass deduced using the new orbital parameters are shown in columns 7 and 8. The dynamical parallaxes obtained by means of the Baize & Romaní algorithm (Heintz 1978) are indicated in column 9 and the individual masses derived from them appear in columns 10 and 11. Docobo & Andrade (2013) introduced both an up-to-date calibration for the cited algorithm as well as the mass–luminosity relation and bolometric correction which we applied in this research. All of the values of the masses are presented with the associated standard errors. Those mass errors were calculated as usual using the propagation of uncertainties. Absolute magnitudes used for calculations were taken from Gray (2005). Both parallaxes are expressed in arcseconds and the masses in solar masses, as usual.

In order to compare each orbit reported in this paper with the previous one, different quality controls are shown in Tables 4 and 5.

Table 2. Ephemerides. Short period orbits marked with ∗ and long period with ∗∗.

WDS	Name	2019		2020		2021		2022		2023	
		θ (°)	ρ arcsec	θ (°)	ρ arcsec	θ (°)	ρ arcsec	θ (°)	ρ arcsec	θ (°)	ρ arcsec
06478+0020	STT157	160.9	0.583	160.1	0.590	159.4	0.597	158.7	0.604	158.0	0.611
07003−2207	FIN334Aa,Ab∗	329.6	0.121	328.8	0.122	328.0	0.124	327.1	0.125	326.3	0.126
07003−2207	FIN334Aa,Ab∗∗	329.5	0.117	328.5	0.116	327.5	0.116	326.5	0.115	325.4	0.114
07013−0906	A671∗	185.4	0.349	184.6	0.352	183.8	0.355	183.0	0.358	182.2	0.361
07013−0906	A671∗∗	5.7	0.356	4.9	0.36	4.2	0.365	3.5	0.369	2.9	0.374
10174−5354	CVN16Aa,Ab	32.7	0.103	87.4	0.103	148.0	0.092	228.6	0.081	310.4	0.091
12155−3106	RST1658	177.5	0.561	182.8	0.544	188.5	0.529	194.5	0.517	200.7	0.508
12572+0818	FIN380	163.2	0.179	163.6	0.159	164.1	0.132	0.165	0.096	167.6	0.04
13044−1316	HU642AB	221.2	0.503	220.9	0.503	220.6	0.503	220.3	0.503	220.0	0.503
14243−3838	RST1785	259.1	0.242	261.4	0.241	263.7	0.24	266.0	0.239	268.3	0.237
16094−3103	I557	198.8	0.265	199.5	0.272	200.2	0.279	200.8	0.285	201.4	0.289
17115−1630	HU169	179.4	0.261	177.7	0.26	176.0	0.259	174.3	0.257	172.6	0.254
17119−0151	LPM629	308.2	0.664	321.2	0.652	334.6	0.643	348.4	0.636	2.4	0.632
17563+0259	A2189	290.4	0.137	292.1	0.143	293.6	0.148	295.1	0.153	296.4	0.158
18464−2755	RST2073	148.7	0.357	147.8	0.365	146.8	0.372	146.0	0.38	145.1	0.388
19035−6845	FIN357	223.5	0.092	179.5	0.115	151.3	0.141	131.8	0.165	116.6	0.182

Table 3. Magnitudes, spectral types, parallaxes, and masses. Short period orbits are marked with ∗ and long period orbits with ∗∗. $\Pi^{\rm Sat}$ column contains *Gaia* or *Hipparcos* values of parallaxes. *H* superscript means that the parallax value comes from *Hipparcos*, no superscript indicates *Gaia*. $\mathcal{M}_{AB}^{\rm Sat}$ shows the total mass derived from these parallaxes with the same superscripts.

WDS *Hipparcos*	Name	m_A	m_B	Sp$_A$	Sp$_B$	$\Pi^{\rm Sat}$ e	$\mathcal{M}_{AB}^{\rm Sat}$ e	$\Pi^{\rm dyn}$ e	$\mathcal{M}_{A}^{\rm dyn}$ e	$\mathcal{M}_{B}^{\rm dyn}$ e
06478+0020	STT157	7.18	9.16	A3	F5	0.00534^{H}	12.514^{H}	–	–	–
HIP 32572						$\pm0.00094^{H}$	$\pm9.583^{H}$			
07003−2207	FIN334	7.04	7.56	B3	B4	0.00155^{H}	35.652^{H}	0.00239	5.301	4.454
HIP 33721	Aa,Ab∗					$\pm0.00052^{H}$	$\pm40.287^{H}$	±0.00049	±4.228	±3.552
07003−2207	FIN334	7.04	7.56	B3	B4	0.00155^{H}	23.505^{H}	0.00202	5.731	4.815
HIP 33721	Aa,Ab∗∗					$\pm0.00052^{H}$	$\pm26.398^{H}$	±0.0004	±4.433	±3.725
07013−0906	A 671∗	9.52	10.12	F4	F7	–	–	0.00825	1.151	1.015
								±0.00049	±0.268	±0.236
07013−0906	A 671∗∗	9.52	10.12	F4	F7	–	–	0.00697	1.247	1.099
								±0.00043	±0.3	±0.265
10174−5354	CVN16	14.45	15.05	M5	M5	0.051	0.233	–	–	–
	Aa,Ab					±0.0003	±0.015			
12155−3106	RST1658	10.17	11.32	K7	M0	0.03464	1.968	0.04326	0.553	0.458
HIP 59780						±0.00076	±0.135	±0.00032	±0.016	±0.013
12572+0818	FIN380	7.36	7.85	F4IV	G2IV	0.00983^{H}	4.517^{H}	0.01191	1.358	1.2
HIP 63221						$\pm0.00071^{H}$	$\pm1.11^{H}$	±0.00056	±0.245	±0.219
13044−1316	HU642	10.41	10.66	F9	G1	0.00756^{H}	1.862^{H}	0.00744	1.003	0.954
HIP 63789	AB					$\pm0.00214^{H}$	$\pm1.688^{H}$	±0.00093	±0.493	±0.469
14243−3838	RST 1785	10.35	10.62	G4	G6	0.0121^{H}	0.724^{H}	0.00888	0.943	0.893
HIP?70410						$\pm0.00158^{H}$	$\pm0.285^{H}$	±0.00013	±0.055	±0.052
16094−3103	I557	7.55	8.35	A5	F0	0.01535	3.552	0.01941	0.968	0.790
						±0.0007	±1.117	±0.00224	±0.433	±0.354
17115−1630	HU169	7.96	8.66	A6	A9	0.02007	0.219	0.00843	1.59	1.365
HIP 84092						±0.00116	±0.041	±0.00022	±0.166	±0.143
17119−0151	LPM 629	11.0	11.2	M3	M3	0.09819^{H}	0.376^{H}	0.07403	0.448	0.429
HIP 84123						$\pm0.01209^{H}$	$\pm0.139^{H}$	±0.00099	±0.024	±0.023
17563+0259	A2189	8.59	9.59	A4	A9	0.00511	3.298	0.00518	1.754	1.403
HIP 87811						±0.00042	±0.912	±0.00026	±0.34	±0.272
18464−2755	RST 2073	10.2	10.3	G2	G3	–	–	0.00828	1.004	0.985
								±0.00051	±0.244	±0.24
19035−6845	FIN357	6.42	6.86	F7	G5	0.01555	3.858	0.01769	1.372	1.247
HIP 93574						±0.00029	±0.233	±0.00016	±0.049	±0.045

Table 4. rms quality controls. Short period orbits marked with ∗ and long period with ∗∗.

WDS	Name	New orbit rms		Previous orbit rms	
		$\Delta\theta$	$\Delta\rho$	$\Delta\theta$	$\Delta\rho$
06478+0020	STT157	3.061	0.031	3.440	0.044
07003−2207	FIN334Aa,Ab∗	1.782	0.003	2.234	0.008
07003−2207	FIN334Aa,Ab∗∗	2.044	0.007	2.234	0.008
07013−0906	A671∗	1.003	0.012	4.023	0.019
07013−0906	A671∗∗	0.725	0.016	4.023	0.019
10174−5354	CVN16Aa,Ab	6.618	0.003	9.023	0.002
12155−3106	RST1658	10.319	0.039	12.432	0.055
12572+0818	FIN380	1.434	0.013	1.72	0.03
13044−1316	HU642AB	5.315	0.058	22.051	0.222
14243−3838	RST1785	3.311	0.016	20.609	0.020
16094−3103	I557	1.105	0.022	1.935	0.048
17115−1630	HU169	2.849	0.01	2.942	0.01
17119−0151	LPM629	4.356	0.052	5.378	0.055
17563+0259	A2189	4.322	0.014	6.127	0.014
18464−2755	RST2073	1.927	0.008	46.093	0.101
19035−6845	FIN357	8.847	0.019	12.898	0.02

First and foremost, we calculated the rms of both coordinates, θ and ρ, using the data weighting scheme given in Docobo & Ling (2003). In this sense, it is necessary to emphasize that the highest weights were assigned to interferometric observations. The results are listed in Table 4.

Table 5 shows the WDS and *Hipparcos* numbers in column 1 and the discovered code (name) in column 2. The author and the year of the previous orbit are found in column 3 and the *Gaia* or *Hipparcos* parallax value in column 4. Both previous and new values for the dynamical parallaxes are in columns 5 and 6, respectively.

Previous speckle data were collected from the USNO Catalogue of Interferometric Measurements of Binary Stars (Hartkopf, McAlister & Mason 2001) and micrometric observations from Worley (1997).

2.1 WDS 06478+0020 (STT 157)

The orbit published by Hartkopf, Mason & Rafferty (2008) has a period of 307.83 yr. However, both the position angle as well as the separation present slight but systematic residuals for all the observations collected since 1999. Previously to that, Heintz (1962, 1973) had calculated the orbit on two different occasions with 265 and 299 yr, respectively. Later observations have suggested that the period may be even larger than previously reported.

Table 5. *Gaia* and *Hipparcos* versus dynamical parallaxes. Π^{Sat} represents *Gaia* or *Hipparcos* values of parallaxes. *H* superscript means *Hipparcos* parallax. No superscript means *Gaia* parallax. Short period orbits marked with ∗ and long periods with ∗∗.

Hipparcos WDS	Name	Previous orbit Author (year)	Π^{Sat} e	Previous orbit Π^{dyn}	New orbit Π^{dyn} e
HIP 32572	STT157	Hartkopf et al.	0.00534^{H}	–	–
06478+0020		(2008)	$\pm0.00094^{H}$		
HIP 33721	FIN334	Docobo & Andrade	0.00155^{H}	0.00207	0.00239
07003−2207	Aa,Ab∗	(2013)	$\pm0.00052^{H}$		±0.00049
HIP 33721	FIN334	Docobo & Andrade	0.00155^{H}	0.00207	0.00202
07003−2207	Aa,Ab∗∗	(2013)	$\pm0.00052^{H}$		±0.0004
	A671∗	Olevic & Cevtkovic	–	0.0083	0.00825
07013−0906		(2005)			±0.00049
	A671∗∗	Olevic & Cevtkovic	–	0.0083	0.00697
07013−0906		(2005)			±0.00043
	CVN16	Bonnefoy	0.051	–	–
10174−5354	Aa,Ab	(2009)	±0.0003		
HIP 59780	RST 1658	Heintz	0.03464	0.04302	0.04326
12155−3106		(1993)	±0.00076		±0.00032
HIP 63221	FIN380	Zirm	0.00983^{H}	0.00732	0.01191
12572+0818		(2008)	$\pm0.00071^{H}$		±0.00056
HIP 63789	HU642	Dommanget	0.00756^{H}	0.0131	0.00744
13044−1316	AB	(1978)	$\pm0.00214^{H}$		±0.00093
HIP 70410	RST1785	Heintz	0.0121^{H}	0.00968	0.00888
14243−3838		(1986)	$\pm0.00158^{H}$		±0.00013
	I557	Zirm	0.01535	0.00952	0.01941
16094−3103		(2013)	±0.00070		±0.00224
HIP 84092	HU169	Docobo & Ling	0.02007	0.00816	0.00843
17115−1630		(2011)	±0.00116		±0.00022
HIP 84123	LPM629	Miles & Mason	0.09819^{H}	0.06865	0.07403
17119−0151		(2016)	$\pm0.01209^{H}$		±0.00099
HIP 87811	A2189	Docobo et al.	0.00511	0.00516	0.00518
17563+0259		(2008)	±0.00042		±0.00026
	RST2073	Seymour et al.	–	0.0261	0.00828
18464−2755		(2002)			±0.00051
HIP 93574	FIN357	Docobo & Andrade	0.01555	0.01942	0.01769
19035−6845		(2013)	±0.00029		±0.00016

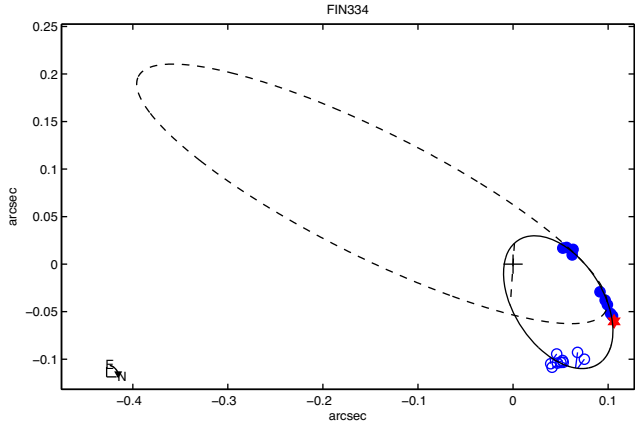

Figure 2. New FIN 344 Aa,Ab∗ with a shorter period than Docobo & Andrade (2013).

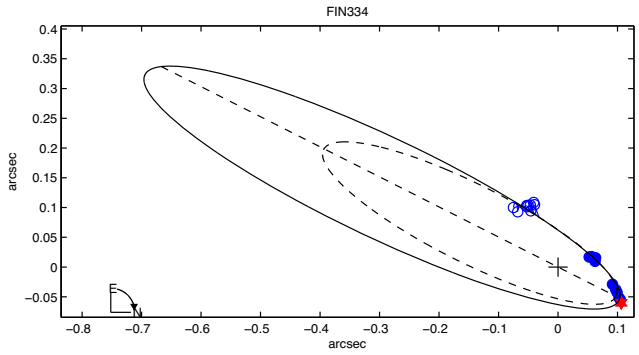

Figure 3. New FIN 344 Aa,Ab∗∗ shows a longer period than Docobo & Andrade (2013).

The SOAR measurement of 2018.2352 (161°, 0.590 arcsec) confirmed said tendency of the Hartkopf et al. (2008) orbit. Therefore, it was necessary to calculate an orbit with a longer period (see Fig. 1).

The newly calculated orbital period of 500 ± 100 yr should still be considered to be provisional although the angle of the position has now diminished by more than 200° (40° with speckle measurements). The quality controls were better than in the past. The composite spectrum is an A5III type which can be broken using spectral decomposition as proposed by Edwards (1976) and separated as an A3III and an F5III. The secondary may also be an F3IV subgiant or an A8V. There is no data concerning the *Gaia* parallax and the *Hipparcos* parallax (0.00534± 0.00094 arcsec) yields a mass that is excessive for the types mentioned. For that reason, it is quite possible that this parallax was underestimated.

2.2 WDS 07003−2207 (FIN 334Aa,Ab)

The binary star, FIN 344Aa,Ab, belongs to the SEE 74AB triple system which is itself orbiting around the mutual centre of mass of the very distant pair, SEE 74CD. Finsen discovered and observed it nine times between 1955 and 1966 using an eyepiece interferometer attached to the 0.7 m telescope of the Union Observatory of Johannesburg. In addition, there were ten speckle measurements with 4 m class telescopes between 1989 and 2018 as well as an unresolved observation of the *Hipparcos* astrometry satellite. Those include four measurements carried out at SOAR between 2009 and 2015, and the latest in 2018 at SOAR as well ($t = 2018.2491$, $\theta = 330\overset{\circ}{.}5$, $\rho = 0.122$ arcsec).

There are four previous solutions for this orbit. The first yields 213.27 yr (Mante 2002), another two give a shorter (105.52 yr) and longer (385.52 yr) period, respectively, (Olevic 2002) and the last solution is of 475.0 yr (Docobo & Andrade 2013). Taking into account the last four speckle measurements, we have calculated two new orbits (with short and long periods of 102.87 yr and 1000.0 yr, respectively) which give better residuals. In all Tables (1–5), we will write FIN 334Aa,Ab∗ for the short period orbit that is shown in Fig. 2 and FIN 334Aa,Ab∗∗ for the long period one (see Fig. 3).

The *Gaia* mission has measured a negative parallax and, although information can be obtained from this data, we have initially used the parallax provided by the new reduction of the *Hipparcos* astrometric data, (1.55 ± 0.52) mas, to estimate a total mass of (36 ± 40) and (24 ± 26) $M_{\odot}$ for the short and long-period orbits, respectively. On the other hand, this system is a B3Vnn spectral type (Houk & Smith-Moore 1988) and both components are equally brilliant (7.2–7.2). Consequently, we could expect a system mass of approximately 15 $M_{\odot}$. Therefore, masses obtained by applying Kepler's Third Law appear too high for a pair of B3 main-sequence stars. In fact, we must note that using the parallax provided by the old reduction of the *Hipparcos* astrometric data (Perryman et al. 1997), (2.46 ± 0.74) mas, we obtain more meaningful (although somewhat low) masses of (8.9 ± 8.9) and (5.9 ± 6.1) $M_{\odot}$ for the short and long-period orbits, respectively. Unfortunately, the low accuracy of the trigonometric parallax does not permit us to decide whether the distance is overestimated or if there are more massive components in the system.

A new orbit, different to that presented in this paper, was calculated simultaneously by Tokovinin (2018c).

2.3 WDS 07013–0906 (A 671)

The first orbit for this pair was calculated by Olevic (2002) and was later improved by Olevic & Cvetkovic (2005), who obtained a period of 352.94 yr.

The four speckle measurements carried out in this century, including that of SOAR in 2018 ($t = 2018.2491$, $\theta = 6\overset{\circ}{.}1$, $\rho = 0.351$ arcsec), produce systematically negative residuals both in theta and in rho with said orbit.

Our solution (P ∼ 342 yr), maintaining the angles of the same quadrants as the previous orbits, clearly improves the rms in theta and rho. There are no parallax measures for the system but the dynamical parallax permits us to obtain reasonably concordant masses associated with the F4 and F7 spectral types. These last were obtained using spectral decomposition as proposed by Edwards (1976), using the value of $\Delta m = 0.6$ provided by Tokovinin, Mason & Hartkopf (2010).

If the position angles measured after 1954 are considered to be in the third quadrant, then it is possible to calculate another solution with an orbital period half that of the other orbit, with good rms as well. In all Tables (1–5) we will write A671∗, Fig. 4, for the short period orbit and A671∗∗ for the long period one, Fig. 5.

2.4 WDS 10174−5354 (CVN 16Aa,Ab)

This low mass X-ray binary has an orbital period of a little more than 5 yr. Its orbit ($P = 5.15$ yr) was first calculated by Bonnefoy et al. (2010) after an infrared speckle register sequence between 2004.177 and 2007.985.

The SOAR measurement (348°.4, 0.102 arcsec) of 2018.2355 yielded a high residual in theta ($\Delta\theta \sim -23\overset{\circ}{.}8$) which suggests a

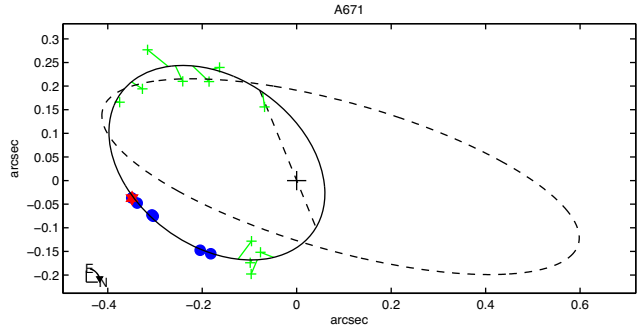

Figure 4. New A671∗ short period orbit.

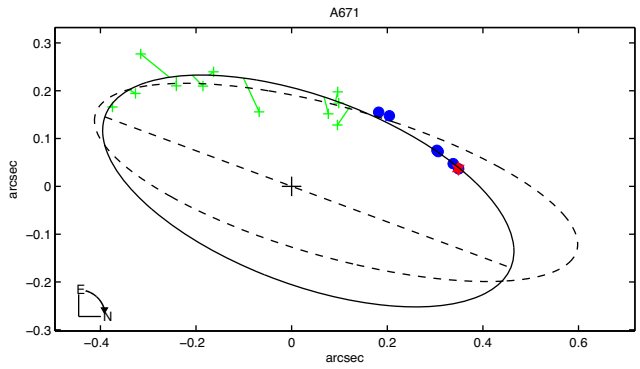

Figure 5. New A671∗∗ long period orbit with the measures after 1954 in the third quadrant.

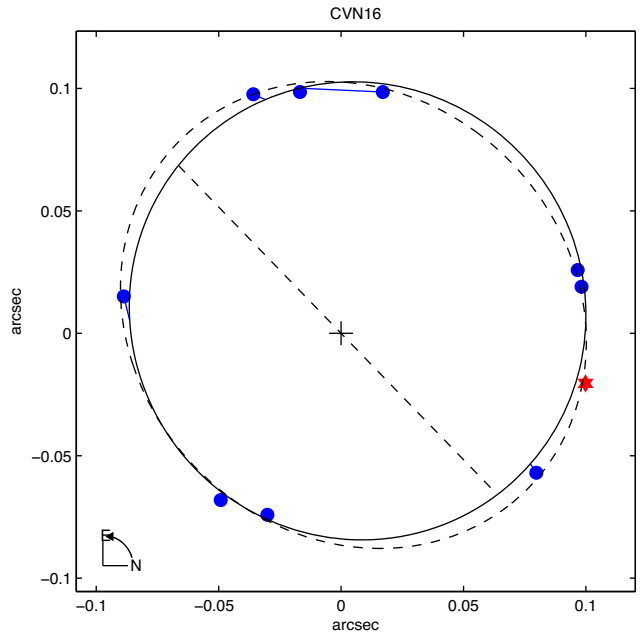

Figure 6. New orbit for CVN 16 AaAb.

somewhat greater orbital period (see Fig. 6). Using $\Delta m = 0.6$, the value obtained in the 2018.2355 observation, the composite magnitude given by Simbad ($m_V = 13.96$ mag) can be separated into 14.45 and 15.05 mag.

Bonnefoy et al. (2010) suggested the M6 ± 1 spectral type.

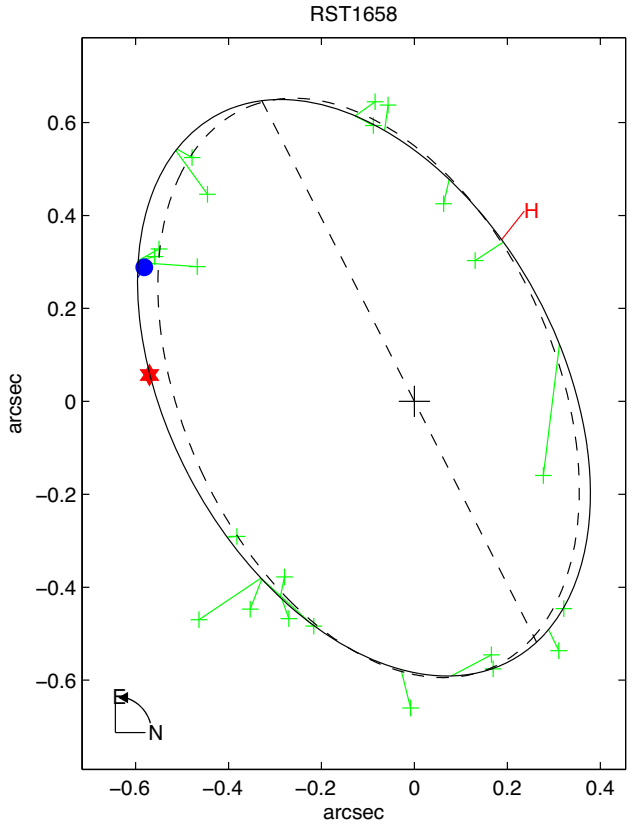

Figure 7. Comparison of the new RST 1658 orbit with the previous.

2.5 WDS 12155–3106 (RST 1658)

Early orbits for this binary were calculated by Heintz (1967, 1981), Starikova (1983), Söderhjelm (1999), and Heintz (1993). Nevertheless, the 2018.2356 SOAR observation (174°.3, 0.573 arcsec) confirmed the residual of the measurement by Tokovinin of 2014.1856 (Tokovinin et al. 2015) with the last orbit by Heintz ($P = 61.20$ yr), demonstrating that the orbital period is slightly greater, as shown in Fig. 7.

With the difference in magnitude given by *Hipparcos*, 1.15 mag, the spectral K7Vk (Gray et al. 2006) decomposition yields K6V-M0V for which the expected mass should be approximately 1.16 $M_\odot$. By means of the dynamical parallax (0.04327 arcsec) and using our values of $P = 62$ yr and $a = 0.68$ arcsec, we calculated masses of (0.55 ± 0.46) $M_\odot$ that are very close to that. On the other hand, the *Gaia* parallax (0.03464 arcsec) yields a substantially greater mass (∼1.97 $M_\odot$).

2.6 WDS 12572+0818 (FIN 380)

Zirm (2008) was the author of the only orbit published for this pair. It was a very eccentric orbit with high inclination and a period of almost 85 yr. The last interferometric measurements including that performed at SOAR in 2018 ($t = 2018.2357$, $\theta = 163°.0$, $\rho = 0.190$ arcsec) showed that the period should be significantly less. Our solution ($P = 55$ yr) reduces it by one-third while, at the same time, the rms are considerably improved in the angle of position as well as the separation.

Although this binary appears as an F5 spectral type in the Simbad data base, there is no doubt that this system was initially catalogued as being composed of subgiants as an F7IV composite spectrum

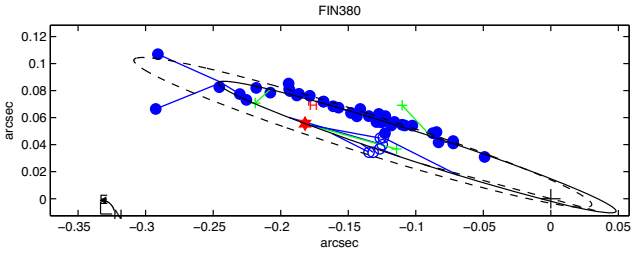

Figure 8. The new orbit for FIN380.

(Harlan 1974). Individual spectra, F4IV and G2IV, can be deduced from the magnitudes of 7.36 and 7.85, respectively, these being obtained from the Tycho magnitude and the differential photometry of the speckle measurements.

No *Gaia* parallax is known and the *Hipparcos* measurement (0.00983± 0.00071 arcsec) may be underestimated as it yields a total mass that is too great. Nevertheless, the masses that are deduced from the dynamical parallax (Docobo & Andrade 2013) are more realistic: 1.34 and 1.20. The apparent orbit of this system is presented in Fig. 8.

Tokovinin (2018d) determined a very similar solution at the same time that we calculated our orbit.

2.7 WDS 13044−1316 (HU 642)

The two SOAR telescope observations of 2018.2361 (221.°4, 0.503 arcsec and 221.°3, 0.507 arcsec) are the first speckle measurements of this system and confirm that the separation between the components continues to increase.

The first orbit calculated by Baize (1958) had a period of 80.35 yr and, later, Dommanget (1978) recalculated it to be 108.11 yr. Our solution has a period of 660 yr and yields a good adjustment in theta but not in rho where too many negative residuals are exhibited. In any case, this binary has a very long period. New observations are necessary in order to precisely determine the epoch of maximum separation (see Fig. 9).

The components of this binary belong to the F9 and G1 main sequence and, for that reason, it is possible to compare the total mass obtained using the *Hipparcos* parallax, 0.00756 arcsec, of 1.862 $M_\odot$ with the other deduced by means of the dynamical parallax, 0.00744 arcsec: 1.95 $M_\odot$ (1.00 + 0.95). *Gaia* data are not available for this pair.

2.8 WDS 14243−3838 (RST 1785)

Costa & Docobo (1983) calculated the first orbit for this binary and obtained a period of 98.2 yr. Later, Heintz (1986) revised it using the 1984.37 observation, reducing the period to 82.8 yr.

The *Hipparcos* and two speckle measurements obtained in Chile (2016.3865, 251.°13, 0.246 arcsec) and (2018.2523, 257°, 0.241 arcsec) showed that the orbital period is greater than that calculated by Heintz. The residuals of the last speckle observation with the Heintz orbit are $\Delta\theta = -22.°5$ and $\Delta\rho = 0.007$ arcsec. The new measure can be seen as a red star in Fig. 10.

There is no *Gaia* parallax and that obtained by *Hipparcos* is overestimated because, in all cases, very low masses are given for the G4–G6 spectral types. In this case, the dynamical parallax seems to be more realistic when it yields masses of 0.94 and 0.89 $M_\odot$ for each component.

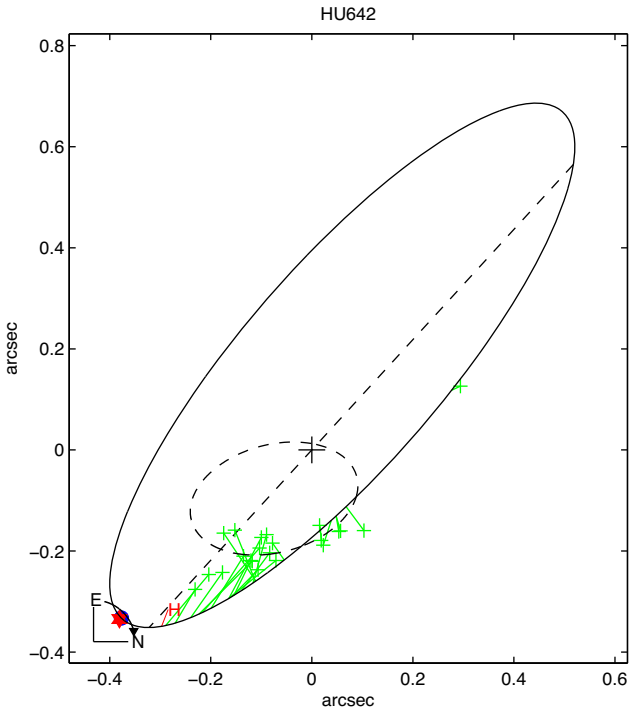

Figure 9. New solution for HU 642.

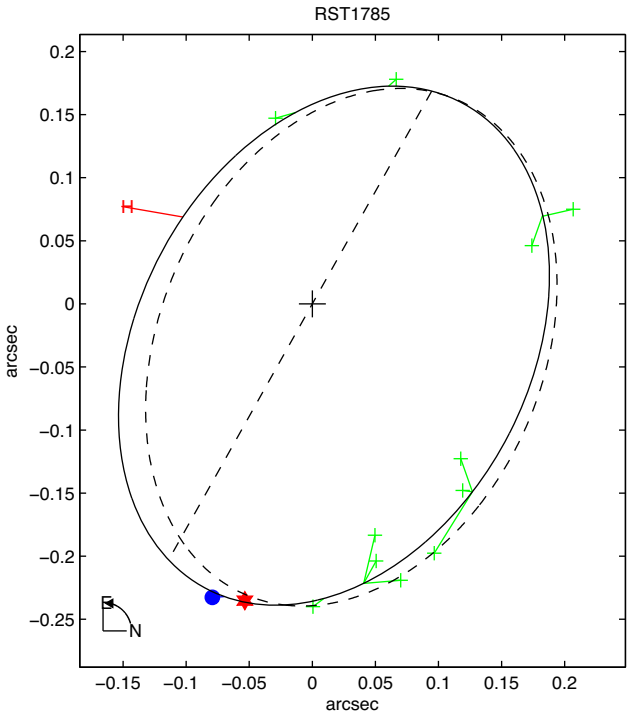

Figure 10. New solution for RST 1785 indicated by SOAR and Hiparcos.

2.9 WDS 16094−3103 (I 557)

The orbit calculated by Zirm (2013) presents a high residual in ρ with respect to the two latest speckle measurements: −0.063 arcsec with that of 2014.3033, (195.°3, 0.216 arcsec), obtained by Tokovinin et al. (2015) and −0.083 arcsec with our SOAR measurement ($t = 2018.2359$, $\theta = 198.°3$, $\rho = 0.262$ arcsec).

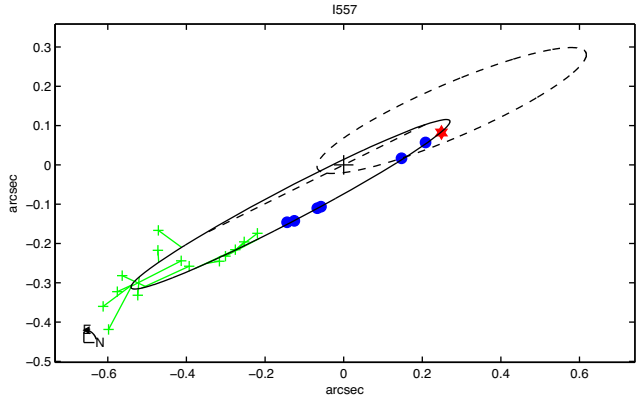

Figure 11. The recalculated orbit for I557.

The Simbad data base indicates a A7IV (Houk 1982) composite spectral type which can be separated into A5IV and F0IV, keeping in mind the value of $\Delta m = 0.8$ provided by Tokovinin et al. (2010, 2015).

Using the *Gaia* parallax, 0.01535± 0.00070 arcsec, the total mass obtained with the orbit presented in this article is (3.55 ± 1.12) $M_{\odot}$, which is in agreement with the previously mentioned spectral types. The previous and new apparent orbits are shown in Fig. 11.

2.10 WDS 17115−1630 (HU 169)

This binary is now completing one revolution since it was discovered in 1900 by Hussey (1900). In Simbad, this pair is listed as a A7V composite spectrum (Houk & Smith-Moore 1988) that, accepting $\Delta m = 0.7$, can be separated into an A6V and an A9V.

The previous orbit (Docobo & Ling 2011) yielded a small residual in theta (+2.°0) and a moderate residual in rho (+ 0.010 arcsec) with the SOAR 2018 observation ($t = 2018.2499, \theta = 181.°2, \rho = 0.2645$ arcsec). Due to that, we decided to calculate a slight improvement.

The sum of the masses which was calculated using the *Gaia* parallax, 0.02007 arcsec, is not realistic. Nevertheless, the *Hipparcos* measurement (0.00829 arcsec) is consistent with the dynamical parallax deduced from this orbit (0.00843 arcsec).

The observations of 1951.60 and 1995.579 have not been considered in the calculation of the rms given the elevated residuals with all of the orbits. See the new orbit compared with the previous in Fig. 12.

2.11 WDS 17119−0151 (LPM 629)

When Baize (1989) calculated the first orbit for this pair of red dwarfs, the period was $P = 33.52$ yr. The orbit was improved to $P = 33.50$ yr by Heintz (1991), $P = 34$ yr by Söderhjelm (1999), and $P = 34.74$ yr by Miles & Mason (2016). This latest orbit presents systematically positive residuals in rho when using the latest speckle measurements which was confirmed by the last SOAR speckle measurement ($t = 2018.2363, \theta = 298.°6, \rho = 0.674$ arcsec). The difference between the previous and the new apparent orbit can be seen in Fig. 13.

The *Gaia* data base contains no parallax information related with this system but the *Hipparcos* parallax is 0.098191 arcsec which appears to be overestimated as the sum of the masses obtained with it, 0.376 M⊙, is too small. A dynamical parallax of 0.07403 arcsec yields more realistic masses (0.448 ± 0.4291) $M_{\odot}$ for M3 spectral types (Stephenson 1986). We used the magnitudes, 11.0–11.2, from

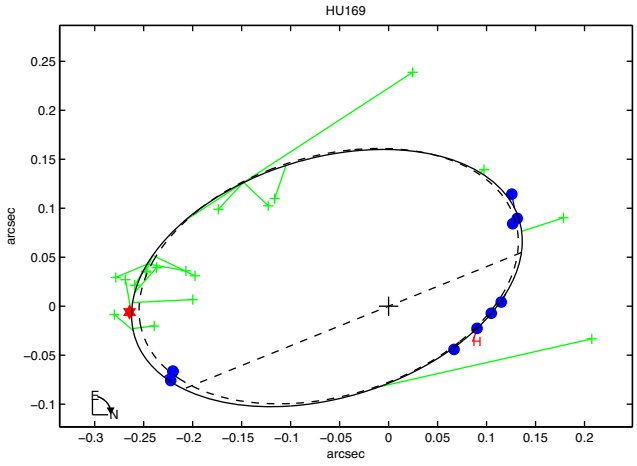

Figure 12. The previous and recalculated orbit for HU 169.

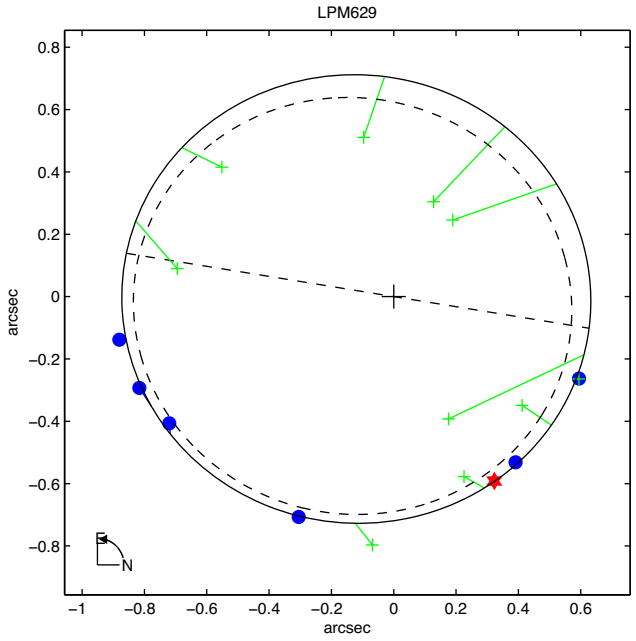

Figure 13. New LPM 629 orbit compared to the previous.

the Washington Double Star Catalogue (Mason et al. 2001) for this calculation.

When we calculated our orbit, Mason et al. (2018) obtained a very similar solution.

2.12 WDS 17563+0259 (A 2189)

Simbad provides a combined magnitude of 8.23 (Tycho) from which the visual magnitudes can be determined for each component, 8.59–9.59, keeping in mind the value of $\Delta m = 1.0$ as given by Tokovinin et al. (2010) and Tokovinin (2012) in both speckle measurements. Early orbits of this system were calculated by Docobo & Costa (1992) and Docobo et al. (2008) with periods of 150 and 154.5 yr, respectively.

The recent measurement obtained with the SOAR telescope (2018.2555, 288.°4, 0.134 arcsec) showed that the orbital period is greater than those solutions. Our new calculation indicates a period of 171.73 yr. The apparent orbit is presented in Fig. 14.

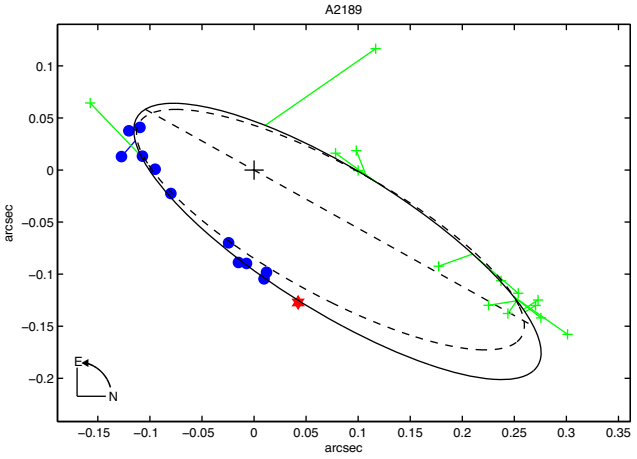

Figure 14. New A2189 orbit.

We have separated the A5IV,V combined spectra (Houk & Swift 1999) into A4V and A9V with the objective of obtaining the dynamical parallax that corresponds to the new orbit. In that way, we obtain 0.00518 arcsec which is in complete agreement with the parallax measured by *Gaia*, 0.00511± 0.00042 arcsec.

2.13 WDS 18464−2755 (RST 2073)

We had only visual measurements that covered a wide arc of the orbit of this binary. The SOAR observations ($t = 2016.3895$, $\theta = 151.^\circ5$, $\rho = 0.34$ arcsec) and ($t = 2018.25$, $\theta = 149.^\circ5$, $\rho = 0.35$ arcsec) are the first speckle measurements for this pair as shown in Fig. 15.

The only orbit for this system had been calculated by Seymour et al. (2002) with the last measurement of 1985.34 and a period of 63.5 yr. More than 30 yr passed without observations since then. Now, with a $\Delta\theta \sim 50^\circ$, we can confirm that it is a long period orbit ($P = 243.5$ yr). There are no parallax measurements for RST 2073 but the dynamical parallax (0.00828 arcsec) yields values of masses that are comparable with the G2–G3 spectral types.

2.14 WDS 19035−6845 (FIN 357)

Since its discovery by Finsen (1959), this binary system has already completed four revolutions until the present. It was measured ten times between 1959 and 1968 by Finsen using his eyepiece interferometer. This system was not observed again until 1991 when the *Hipparcos* mission carried out a new measure. However, we had to wait until the last decade to have observations made with a large telescope. These include measurements at SOAR in 2008, 2015, and the latest, in 2018 ($t = 2018.2554$, $\theta = 266.^\circ4$, $\rho = 0.0866$ arcsec).

This system has been classified as G0IV (Houk & Cowley 1975) as well as F8V (Malaroda 1975) and shows a *Hipparcos* difference of magnitudes of 0.381 ± 0.153. Thus, we could expect a system mass between 2 and 3 $M_\odot$.

The previous orbit shows relatively large residuals with the last speckle measurements (Docobo & Andrade 2013), thus we recalculated it. As a result, the new orbital elements along with the *Gaia* parallax, (15.55 ± 0.29) mas, yield a mass of (3.86 ± 0.23) $M_\odot$. The apparent orbit of this system is presented in Fig. 16.

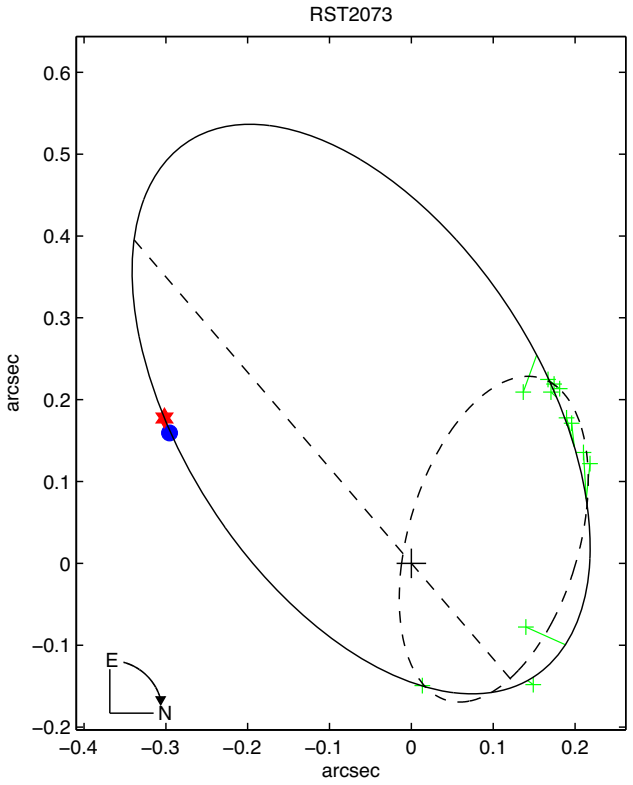

Figure 15. New orbit for RST 2073 according to the recent speckle observations.

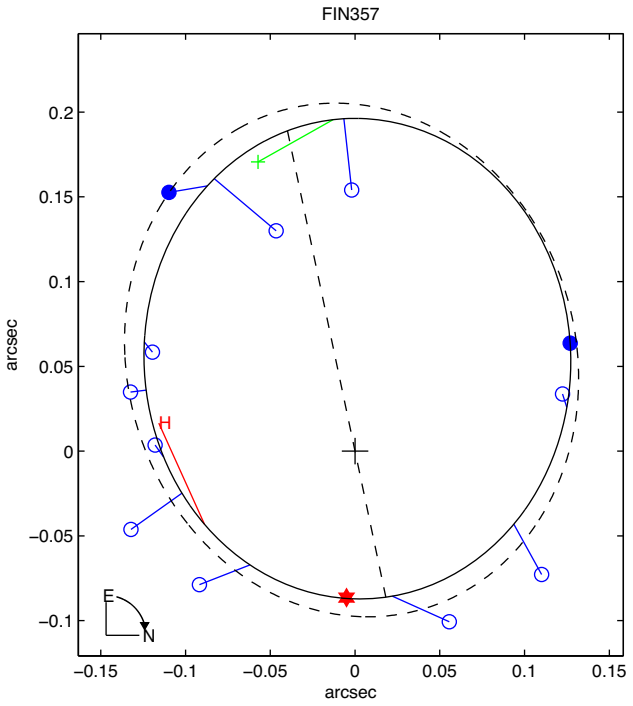

Figure 16. New and previous solution for FIN 357.

Table 6. Absolute magnitudes and luminosities obtained from the dynamical parallax.

Star	M_{VA}	M_{VB}	L_A ($L_\odot$)	L_B ($L_\odot$)
FIN334∗	−1.07	−0.55	836.19	356.57
FIN334∗∗	−1.43	−0.91	1433.11	655.86
A671∗	4.10	4.70	1.85	1.11
A671∗∗	3.74	4.34	2.58	1.51
RST1658	8.35	9.50	0.09	0.05
FIN380	2.74	3.23	6.20	4.02
HU642	4.77	5.02	1.05	0.84
RST1785	5.09	5.36	0.79	0.62
I557	3.99	4.79	2.05	1.02
HU169	2.59	3.29	7.13	3.82
LPM629	10.35	10.55	0.032	0.03
A2189	2.16	3.16	10.56	4.26
RST2073	4.79	4.89	1.02	0.94
FIN357	2.66	3.10	6.68	4.50

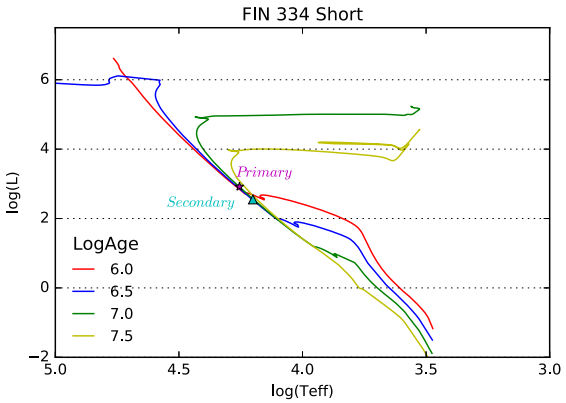

Figure 17. HR diagram for FIN334, short period.

3 LUMINOSITIES AND AGES

We may now obtain the absolute magnitudes of the components by means of the dynamical parallax and calculate the luminosities by using the formula (Torres 2010)

$$\log\frac{L}{L_\odot} = -0.4(M_V - V_\odot - 31.572 + (BC_V - BC_\odot)) \quad (1)$$

where L is the luminosity, M_V is the absolute V magnitude of the star, $V_\odot$ is the apparent visual magnitude of the Sun, and BC_V and $BC_\odot$ are the bolometric corrections of the star and the Sun in the V band, respectively. We adopted the value of $V_\odot$ from Torres (2010) and the bolometric corrections from Straizys & Kuriliene (1981). The results can be seen in Table 6, where the name of the star appears in the first column. An asterisk indicates the short period orbit whereas two asterisks correspond to the long period orbit. The second and third columns show the absolute magnitudes of the components, and the fourth and fifth correspond to the luminosities.

We could not apply this methodology for STT157 because the Baize–Romani algorithm is not calibrated for class III giants. In the case of CVN16 Aa,Ab, the lack of magnitude difference measurements in the visual band prevented us from obtaining the absolute magnitudes.

In order to obtain orientative information related to the age of these systems, we selected their metallicity values from different

Table 7. Temperature and metallicity.

Hipparcos WDS	Name	Metalicity	Catalogue	$T_{\rm eff}$ Log	$v/v_{\rm crit}$
HIP 32572	STT157	–	–	–	–
06478 + 0020					
HIP 07003−2207	FIN334	0.0	–	4.255	0.4
07003−2207	Aa,Ab			4.2006	
	A671	0.18	Ammons et al.	3.8273	0.0
07013−0906			(2006)	3.8024	
	CVN16	–	–	–	–
10174−5354	Aa,Ab				
HIP 59780	RST 1658	0.0	–	3.64147	0.0
12155−3106				3.62448	
HIP 63221	FIN380	0.27	Anderson et al.	3.829	0.0
12572+0818			(2012)	3.764	
HIP 63789	HU642	-0.26	Ammons et al.	3.782	0.0
13044−1316	AB		(2006)	3.7694	
HIP 70410	RST1785	-0.43	Ammons et al.	3.7589	0.0
14243−3838			(2006)	3.7458	
	I557	0.0	–	3.9194	0.0
16094−3103				3.856	
HIP 84092	HU169	0.0	–	3.90956	0.0
17115−1630				3.8808	
HIP 84123	LPM629	-0.22	Gaidos et al.	3.5966	0.0
17119−0151			(2014)	3.5966	
HIP 87811	A2189	0.0	–	3.937	0.0
17563+0259				3.8808	
	RST2073	0.2	Ammons et al.	3.76425	0.0
18464−2755			(2006)	3.758	
HIP 93574	FIN357	0.33	Anderson et al.	3.76425	0.0
19035−6845			(2012)	3.7526	

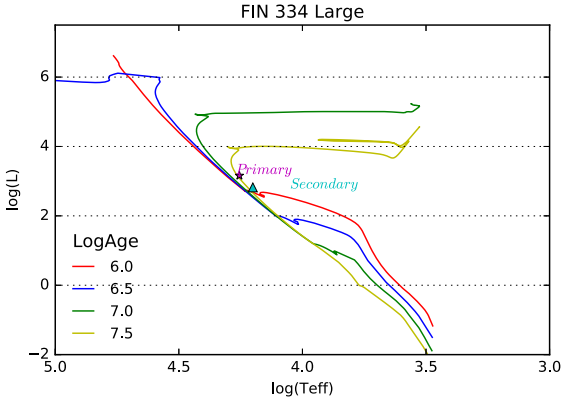

Figure 18. HR diagram for FIN334, long period.

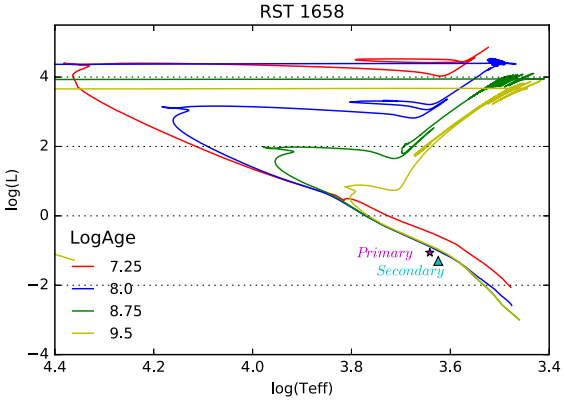

Figure 21. HR diagram for RST1658.

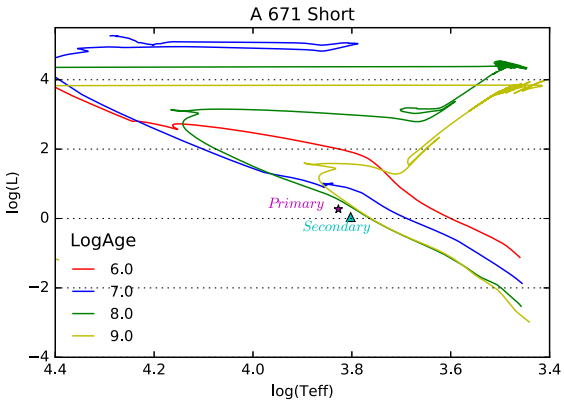

Figure 19. HR diagram for A671, short period.

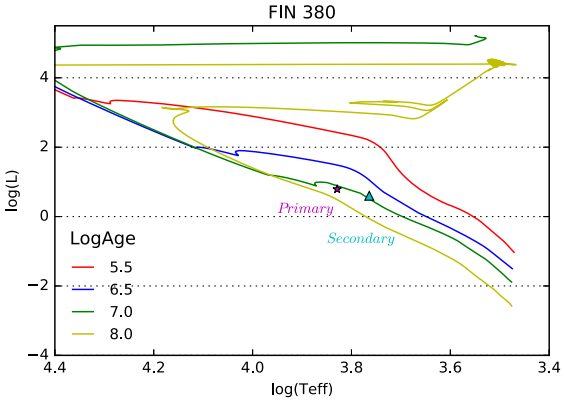

Figure 22. HR diagram for FIN380.

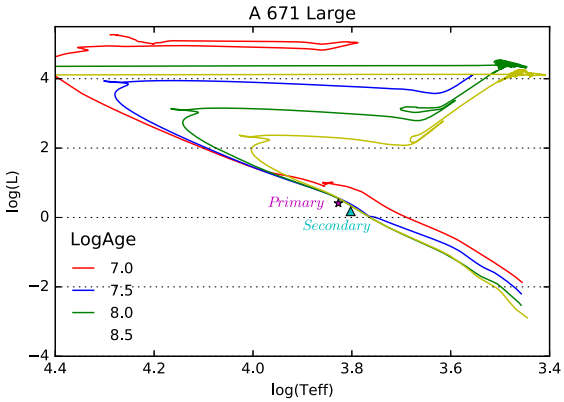

Figure 20. HR diagram for A671, long period.

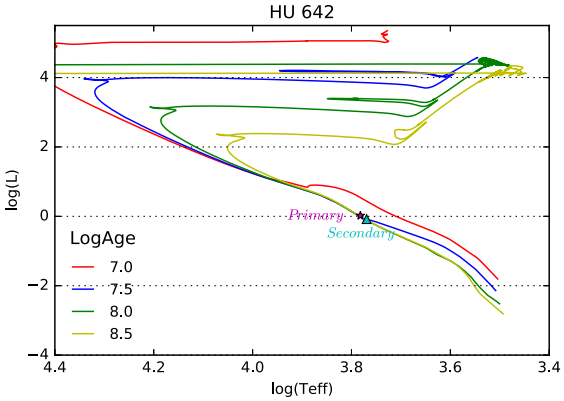

Figure 23. HR diagram for HU642.

catalogues (Ammons et al. 2006; Anderson & Francis 2012; Gaidos et al. 2014). We also needed to use the relations between spectral types and effective temperatures provided by Gray (2005). The values used to calculate the isochrones can be seen in Table 7. In all cases but FIN 334, the $v/v_{\rm crit}$ value used was zero. The isochrones were provided by MESA Isochrones and Stellar Tracks (Paxton et al. 2011, 2013, 2015; Choi et al. 2016; Dotter 2016). We have plotted the components of the systems in HR diagrams (see Figs 17–30), showing also the isochrones of the most probable ages of the system. Although the data do not allow us to assure a definitive value for the ages of some of the systems, mainly due to the relatively large uncertainties in the orbital parameters, we can see that the

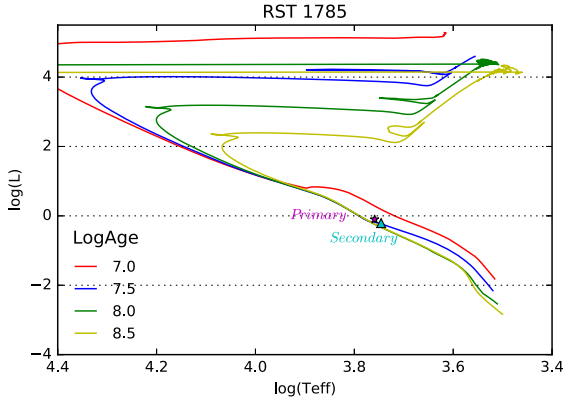

Figure 24. HR diagram for RST1785.

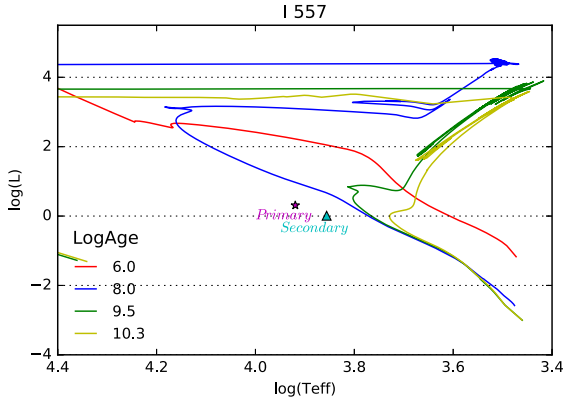

Figure 25. HR diagram for I557.

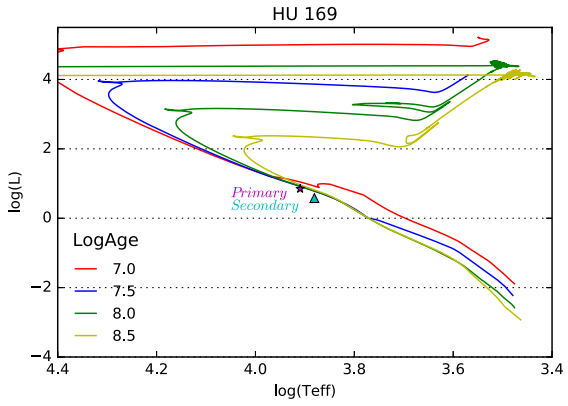

Figure 26. HR diagram for HU169.

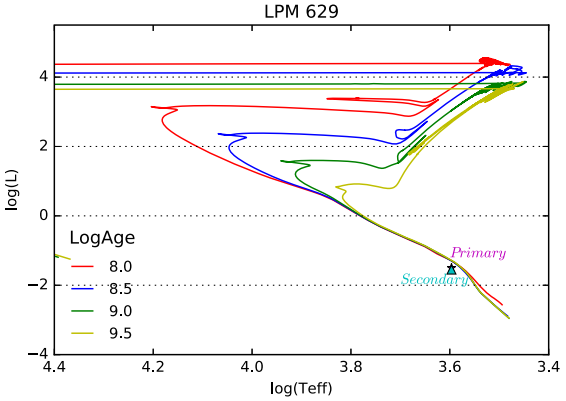

Figure 27. HR diagram for LPM629.

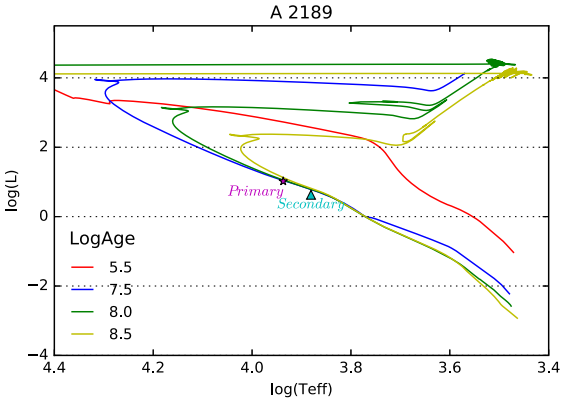

Figure 28. HR diagram for A2189.

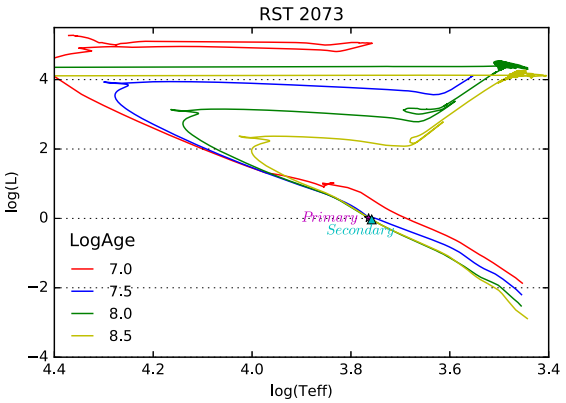

Figure 29. HR diagram for RST2073.

calculated luminosities are coherent with the coevolution of the systems, meaning that both components have the same origin.

4 CONCLUSIONS

As mentioned, the speckle interferometry SOAR campaigns have being very productive in fields related with binary and multiple systems. Since 2008, it also permitted the discovery and tracking of binaries that are of special astrophysical interest. In terms of this study, the observation campaign that was carried out in 2018 March represented the continuation of a collaboration between the teams of RAM and JAD that began in 2015. This is the second paper produced for this project.

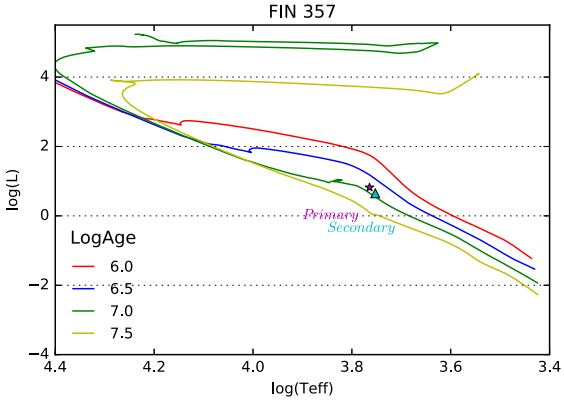

Figure 30. HR diagram for FIN357.

The binaries proposed for observation were selected according to several criteria: no observations for many years, previous orbits recorded with increasing residuals, no speckle observations, etc. The orbits and the respective masses of the systems have been improved and, in two cases (A 671 and FIN 344Aa,Ab) two different orbits have been calculated for the same binary due to a possible flip of the position angles. The first speckle measurements of the HU 642, RST 1785, and RST 2073 binaries were performed between 2016 and 2018. It has allowed to calculate more precise orbits for these systems.

ACKNOWLEDGEMENTS

The authors thank Andrei Tokovinin for his collaboration with speckle runs carried out at Southern Astrophysical Research telescope in 2018 March, as well as for his review of this manuscript.

We must also express our deep gratitude to the operator and engineer teams of Southern Astrophysical Research telescope that were involved with the observation campaigns.

We would also like to thank the referee, A. E. Lynas-Gray, for numerous comments and suggestions on the original manuscript, which greatly improved the paper.

This paper was supported by the Spanish 'Ministerio de Economía, Industria y Competitividad' under the Project AYA-2016-80938P (AEI/FEDER, UE) and by the 'Xunta de Galicia' under the Rede IEMath-Galicia, ED341DR, 2016/022 grant.

RAM acknowledges support from the Chilean Centro de Excelencia en Astrofísica y Tecnologías Afines (CATA) BASAL PFB/06, from the Fondo Nacional de Desarrollo Científico y Tecnológico/Comisión Nacional de Investigación Científica y Tecnológica (FONDECYT/CONICYT) grant Nro. 1170854, and from the Chilean Time Allocation Committee (CNTAC) through program CN2018A-1.

This work used the SIMBAD service operated by the Centre des Données Stellaires (Strasbourg, France), bibliographic references from the Astrophysics Data System maintained by SAO/NASA, the Washington Double Star Catalog maintained at USNO, and the Catalog of Orbits and Ephemerides of Visual Double Stars (OARMAC) maintained at the Ramon María Aller Astronomical Observatory.

This work has made use of data from the European Space Agency (ESA) mission *Gaia* (https://www.cosmos.esa.int/gaia), processed by the *Gaia* Data Processing and Analysis Consortium (DPAC, https://www.cosmos.esa.int/web/gaia/dpac/consortium). Funding for the DPAC has been provided by national institutions, in particular, the institutions participating in the *Gaia* Multilateral Agreement.

This study is based on observations obtained at the Southern Astrophysical Research (SOAR) telescope, which is joint project of the Ministério da Ciência, Tecnologia, e Inovâao (MCTI) da República Federativa do Brasil, the U.S.National Optical Astronomy Observatory (NOAO), the University of North Carolina at Chapel Hill (UNC), and Michigan State Univeristy (MSU).

REFERENCES

Ammons S. M., Robinson S. E., Strader J., Laughlin G., Fischer D., Wolf A., 2006, ApJ, 638, 1004
Anderson E., Francis C., 2012, Astron. Lett., 38, 331
Baize P., 1958, JO, 41, 163
Baize P., 1989, A&AS, 78, 125
Bonnefoy M. et al., 2010, in Montmerle T., Ehrenreich D., Lagrange A. M., eds, Physics and Astrophysics of Planetary Systems, EAS Publ. Ser, p. 95
Choi J., Dotter A., Conroy C., Cantiello M., Paxton B., Johnson B. D., 2016, ApJ, 823, 102
Costa J. M., Docobo J. A., 1983, Circ. d'Inf., 91, 1
Docobo J. A., 1985, Celest. Mech., 36, 143
Docobo J. A., 2012, in Arenou F., Hestroffer D., eds, Proc. Orbital Couples: Pas de Deux in the Solar System and the Milky Way, p. 119
Docobo J. A., Andrade M., 2013, MNRAS, 428, 321
Docobo J. A., Costa J. M., 1992, ApJS, 82, 323
Docobo J. A., Ling J. F., 2003, A&A, 409, 989
Docobo J. A., Ling J. F., 2011, IAU Comm. 26 Inform. Circular (IAUDS), 175, 3
Docobo J. A., Tamazian V. S., Andrade M., Ling J. F., Balega Y. Y., Lahulla J. F., Maximov A. A., 2008, AJ, 135, 1803
Docobo J. A., Tamazian V. S., Campo P. P., 2018, MNRAS, 476, 2792
Dommanget J., 1978, Bull. Astron. Obs. R. Belg., 9, 47
Dotter A., 2016, ApJS, 222, 8
Edwards T. W., 1976, AJ, 81, 245
ESA ed., 1997, The HIPPARCOS and TYCHO catalogues. Astrometric and photometric star catalogues derived from the ESA HIPPARCOS Space Astrometry Mission, ESA SP-1200
Finsen W. S., 1959, Mon. Notes Astron. Soc. South. Afr., 18, 114
Gaia Collaboration, 2018, A&A, 616, A1
Gaia Collaboration, 2016, A&A, 595, A2
Gaidos E. et al., 2014, MNRAS, 443, 2561
Gray D. F., 2005, The Observation and Analysis of Stellar Photospheres. Cambridge University Press, Cambridge
Gray R. O., Corbally C. J., Garrison R. F., McFadden M. T., Bubar E. J., McGahee C. E., O'Donoghue A. A., Knox E. R., 2006, AJ, 132, 161
Harlan E. A., 1974, AJ, 79, 682
Hartkopf W. I., McAlister H. A., Mason B. D., 2001, AJ, 122, 3480
Hartkopf W. I., Mason B. D., Rafferty T. J., 2008, AJ, 135, 1334
Heintz W. D., 1962, Veroeff. Sternw. Munchen, 5, 135
Heintz W. D., 1967, Veroff. Sternw. Munchen, 7, 29
Heintz W. D., 1973, AJ, 78, 208
Heintz W. D., 1978, Double Stars, revised edition, Dordrecht, D. Reidel Publishing Co., Geophysics and Astrophysics Monographs, 15, p. 184
Heintz W. D., 1981, ApJS, 45, 559
Heintz W. D., 1986, A&AS, 64, 1
Heintz W. D., 1991, A&AS, 90, 311
Heintz W. D., 1993, A&AS, 98, 209
Houk N., 1982, Michigan Catalogue of Two-dimensional Spectral Types for the HD stars. Volume 3. Declinations −40°0 to −26°0. Departments of Astronomy, University of Michigan, Ann Arbor, MI (USA), 12, p. 390
Houk N., Cowley A. P., 1975, University of Michigan Catalogue of two-dimensional spectral types for the HD stars. Volume I. Declinations −90° to −53°0, Departments of Astronomy, University of Michigan, Ann Arbor, MI (USA), 19, p. 452

Houk N., Smith-Moore M., 1988, Michigan Catalogue of Two-dimensional Spectral Types for the HD Stars. Volume 4, Declinations −26°0 to −12°0, Departments of Astronomy, University of Michigan, Ann Arbor, MI (USA)
Houk N., Swift C., 1999, Michigan Spectral Survey, Vol. 5. Ann Arbor, Dep. Astron., Univ. Michigan, Michigan
Hussey W. J., 1900, AJ, 21, 35
Labeyrie A., 1970, A&A, 6, 85
Malaroda S., 1975, AJ, 80, 637
Mante R., 2002, IAU Commission on Double Stars, p. 148
Mason B. D., Wycoff G. L., Hartkopf W. I., Douglass G. G., Worley C. E., 2001, AJ, 122, 3466
Mason B. D., Hartkopf W. I., Miles K. N., Subasavage J. P., Raghavan D., Henry T. J., 2018, AJ, 155, 215
Mendez R. A., Claveria R. M., Orchard M. E., Silva J. F., 2017, AJ, 154, 187
Miles S. K. N., Mason B. D., 2016, IAU Comm. G1 Inform. Circular (IAUDS), 190, 1
Olevic D., 2002, IAU Commission on Double Stars, p. 148
Olevic D., Cvetkovic Z., 2005, Rev. Mex. Astron. Astrofis., 41, 17
Paxton B., Bildsten L., Dotter A., Herwig F., Lesaffre P., Timmes F., 2011, ApJS, 192, 3
Paxton B. et al., 2013, ApJS, 208, 4
Paxton B. et al., 2015, ApJS, 220, 15
Perryman M. A. C. et al., 1997, A&A, 323, L49
Seymour D. M., Mason B. D., Hartkopf W. I., Wycoff G. L., 2002, AJ, 123, 1023
Söderhjelm S., 1999, A&A, 341, 121
Starikova G. A., 1983, Sov. Astron. Lett., 9, 189
Stephenson C. B., 1986, AJ, 92, 139
Straizys V., Kuriliene G., 1981, Ap&SS, 80, 353
Tokovinin A., 2012, AJ, 144, 56
Tokovinin A., 2016, AJ, 152, 138
Tokovinin A., 2017, AJ, 154, 110
Tokovinin A., 2018a, PASP, 130, 035002
Tokovinin A., 2018b, AJ, 155, 160
Tokovinin A., 2018c, IAU Comm. G1 Inform. Circular (IAUDS), 195, 1
Tokovinin A., 2018d, IAU Comm. G1 Inform. Circular (IAUDS), 195, 2
Tokovinin A., Cantarutti R., 2008, PASP, 120, 170
Tokovinin A., Mason B. D., Hartkopf W. I., 2010, AJ, 139, 743
Tokovinin A., Mason B. D., Hartkopf W. I., Mendez R. A., Horch E. P., 2015, AJ, 150, 50
Tokovinin A., Cantarutti R., Tighe R., Schurter P., Martinez M., Thomas S., van der Bliek N., 2016, PASP, 128, 125003
Tokovinin A., Mason B. D., Hartkopf W. I., Mendez R. A., Horch E. P., 2018, AJ, 155, 235
Torres G., 2010, AJ, 140, 1158
van Leeuwen F., 2007, A&A, 474, 653
Wenger M. et al., 2000, A&AS, 143, 9
Worley C. E., 1997, Balt. Astron., 6, 248
Zirm H., 2008, IAU Commission on Double Stars, 166, 1
Zirm H., 2013, IAU Comm. 26 Inform. Circular (IAUDS), 180, 2

This paper has been typeset from a TEX/LATEX file prepared by the author.